

# The role of Ni and Co promoters in the simultaneous HDS of dibenzothiophene and HDN of amines over Mo/ $\gamma$ -Al<sub>2</sub>O<sub>3</sub> catalysts

Marina Egorova, Roel Prins \*

*Institute of Chemical and Bioengineering, ETH Zurich, 8093 Zurich, Switzerland*

Received 15 December 2005; revised 7 April 2006; accepted 10 April 2006

## Abstract

2-Methylpyridine and 2-methylpiperidine strongly inhibited the hydrogenation pathway in the hydrodesulfurization (HDS) of dibenzothiophene (DBT) and 4,6-dimethyldibenzothiophene over sulfided NiMo/ $\gamma$ -Al<sub>2</sub>O<sub>3</sub>, CoMo/ $\gamma$ -Al<sub>2</sub>O<sub>3</sub>, and Mo/ $\gamma$ -Al<sub>2</sub>O<sub>3</sub> catalysts at 340 °C, 4.8 MPa H<sub>2</sub>, and 35 kPa H<sub>2</sub>S. The direct desulfurization (DDS) pathway was inhibited by both amines over the Mo and CoMo catalysts as well, but the NiMo catalyst showed a promotion effect in the HDS of DBT at 300 °C and at low partial amine pressure. Experiments with other amines showed that only the more basic and stable heterocyclic amines promoted the DDS pathway of DBT over NiMo. This promoting effect of amines on NiMo is explained by the special location of the Ni promoter atoms, on the metal edge of the MoS<sub>2</sub> particles with low sulfur coverage. The perpendicular adsorption of amines hinders especially the  $\pi$  adsorption of DBT and 4,6-dimethyldibenzothiophene and thus the hydrogenation pathway, whereas the filling of sulfur vacancies by H<sub>2</sub>S inhibits the DDS pathway.

© 2006 Elsevier Inc. All rights reserved.

**Keywords:** Hydrodesulfurization; Dibenzothiophene; 4,6-Dimethyldibenzothiophene; Hydrodenitrogenation; 2-Methylpyridine; 2-Methylpiperidine; Promoting effect; Hydrogenation; Direct desulfurization

## 1. Introduction

European environmental regulations currently allow no more than 50 ppm sulfur in gasoline and diesel fuel and most likely will require a further reduction by the end of the decade. Deep hydrodesulfurization (HDS) technology must be implemented to attain this low level of sulfur. Nitrogen-containing compounds are harmful in deep HDS, because they inhibit the HDS of sulfur-containing compounds through competitive adsorption [1–3]. In the past, this was not a problem, because the amount of nitrogen-containing molecules in desulfurized naphtha and gas oil was still much smaller than that of the remaining sulfur-containing molecules. At the low sulfur level currently required, however, nitrogen-containing compounds compete with the sulfur-containing molecules for the sites on the catalyst surface. Consequently, knowledge of the mutual

effects of HDS and hydrodenitrogenation (HDN) is becoming more important.

Dibenzothiophene molecules with alkyl groups in the 4 and 6 positions, adjacent to the sulfur atom, are among the most difficult molecules to desulfurize and create difficulties in deep HDS [3,4]; thus, 4,6-dimethyldibenzothiophene (4,6-DMDBT) is often used as model molecule in HDS studies. The HDS of 4,6-DMDBT goes through two reaction pathways: direct desulfurization (DDS) by hydrogenolysis of the C–S bonds, which leads to the formation of 3,3'-dimethylbiphenyl, and hydrogenation (HYD) to hydrogenated intermediates, followed by desulfurization to 3,3-dimethylcyclohexylbenzene and 3,3'-dimethylbicyclohexyl. Several research groups have reported that nitrogen-containing molecules inhibit the DDS and the HYD pathways of the HDS of dibenzothiophene (DBT) to different extents; the HYD route is strongly suppressed, whereas the DDS route is less seriously affected [2,5–7]. In some cases, the DDS conversion was enhanced, even though the total conversion of the sulfur-containing compounds decreased [2,6,7]. Nagai even reported an enhanced overall conversion of DBT

\* Corresponding author.

E-mail address: [roel.prins@chem.ethz.ch](mailto:roel.prins@chem.ethz.ch) (R. Prins).

over NiMo/Al<sub>2</sub>O<sub>3</sub> and NiW/Al<sub>2</sub>O<sub>3</sub> catalysts in the presence of acridine [5,8].

In previous work at 340 °C and 4.8 MPa H<sub>2</sub>, in the presence of 35 kPa H<sub>2</sub>S, we observed a strong inhibition of the HYD pathway of the HDS of DBT by 2-methylpyridine (2-MPy) and 2-methylpiperidine (2-MPiper) and enhancement of the DDS pathway [9]. This enhancement is not due to a real promotion effect, but rather results from the higher amount of DBT available for the DDS pathway because of the suppression of the HYD pathway. This was confirmed by calculations in which it was assumed that the rate constant of the DDS route was not affected at low concentrations of N-compounds and that the HYD pathway was totally blocked. At the lower temperature of 300 °C, the inhibitory effect of 2-MPy and 2-MPiper on the hydrogenation pathway of the HDS of DBT was increased [10], but the influence of 2-MPiper on the DDS pathway turned into a real promotion effect at low amine concentrations. Not only the formation of biphenyl, but also the conversion of DBT, increased at low partial pressures of 2-MPiper. At high partial pressures of 2-MPiper, inhibition was observed.

To clarify these inhibiting and promoting effects and to gain a better understanding of the role of the catalyst structure and the promoter atom, we extended our investigation of the NiMo catalyst to a series of nitrogen-containing molecules with cyclic as well as acyclic structure, to 4,6-DMDBT, and to sulfided Mo and CoMo catalysts. The results demonstrate that whereas amines inhibit the HYD pathway over all catalysts, the influence on the DDS pathway depends on the catalyst. This is explained by the position of the Co and Ni atoms at the metal and sulfur edges of the MoS<sub>2</sub> crystallites.

## 2. Experimental

Mo/γ-Al<sub>2</sub>O<sub>3</sub>, NiMo/γ-Al<sub>2</sub>O<sub>3</sub>, and CoMo/γ-Al<sub>2</sub>O<sub>3</sub> catalysts with 8 wt% Mo and 0 or 3 wt% promoter (Ni or Co) were prepared by successive incipient wetness impregnation of γ-Al<sub>2</sub>O<sub>3</sub> (Condea; pore volume, 0.5 cm<sup>3</sup> g<sup>-1</sup>; specific surface area, 230 m<sup>2</sup> g<sup>-1</sup>) with an aqueous solution of (NH<sub>4</sub>)<sub>6</sub>Mo<sub>7</sub>O<sub>24</sub> · 4H<sub>2</sub>O, followed (for the promoted catalysts) by an aqueous solution of Ni(NO<sub>3</sub>)<sub>2</sub> · 6H<sub>2</sub>O or Co(NO<sub>3</sub>)<sub>2</sub> · 6H<sub>2</sub>O (all from Aldrich). After each impregnation step, the catalysts were dried in air at ambient temperature for 4 h and then in an oven at 120 °C for 15 h and finally calcined at 500 °C for 4 h. Organic chemicals were used as purchased from Fluka (DBT, toluene, dodecane, heptane, 2-MPy, 2-MPiper, piperidine, dipentylamine, N,N-dimethylaniline), Acros (4,6-DMDBT, 2-methylpyrrolidine), and TCI (neopentylamine).

Reactions were carried out in a continuous mode in a fixed-bed Inconel reactor. The catalyst (0.05 g, diluted with 8 g of SiC) was sulfided in situ with 10% H<sub>2</sub>S in H<sub>2</sub> at 400 °C and 1.0 MPa for 4 h. After sulfidation, the pressure was increased to 5.0 MPa, the temperature was decreased to reaction temperature, and the liquid reactant was fed to the reactor, as described elsewhere [9]. The HDS and HDN experiments were performed at 300 and 340 °C. The gas-phase feed consisted of 130 kPa toluene (solvent for DBT and 4,6-DMDBT), 8 kPa dodecane (reference for DBT, 4,6-DMDBT, and their deriva-

tives in the GC analysis), 1 kPa DBT or 4,6-DMDBT, 0 or 10 kPa heptane (reference for amines and their derivatives), 0–10 kPa amine, 35 kPa H<sub>2</sub>S, and 4.8 MPa H<sub>2</sub>. The partial pressure of the sulfur-containing molecules in the gas feed in the present study was lower than that in the work of Nagai and Satterfield [2,5–8], but we always added gaseous H<sub>2</sub>S to the feed to maintain the catalyst in the sulfided state. The ratio of sulfur to nitrogen-containing compounds corresponded to that used in the work of Nagai and Satterfield. The reaction products were analyzed by off-line GC, as described elsewhere [9]. Weight time was defined as  $\tau = w_{\text{cat}}/n_{\text{feed}}$ , where  $w_{\text{cat}}$  denotes the catalyst weight and  $n_{\text{feed}}$  the total molar flow to the reactor (1 g min/mol = 0.15 g h/l). The weight time ( $\tau$ ) was changed by varying the flow rates of the liquid and the gaseous reactants, while keeping their ratio constant. The reaction was stable after 3–4 h; during the 2 weeks of operation, there was almost no deactivation of the catalyst.

## 3. Results

### 3.1. HDS of DBT at 340 °C

The effect of 2-MPy and 2-MPiper on the HDS of DBT was studied at 340 °C and 35 kPa H<sub>2</sub>S over Mo/γ-Al<sub>2</sub>O<sub>3</sub> and CoMo/γ-Al<sub>2</sub>O<sub>3</sub> catalysts. The influence of both amines was similar; therefore, we present figures only for the effect of 2-MPy. Over Mo/γ-Al<sub>2</sub>O<sub>3</sub>, the HDS of 1 kPa DBT was already strongly suppressed at 1 kPa of the amine (Fig. 1). The conversion of DBT at  $\tau = 5$  g min/mol decreased by a factor of 6.8 in the presence of 2-MPy (Table 1) and 9.4 in the presence of 2-MPiper (Table 2). The conversion further decreased when the partial pressure of the amine was increased to 6 kPa (Fig. 1) with reduction factors of 10.5 and 11.5, respectively. However, the HYD pathway was much more inhibited than the DDS pathway, by factors of 12 (HYD) and 3 (DDS) at 1 kPa 2-MPy (Table 1) and by factors of 15 (HYD) and 4 (DDS) at 1 kPa 2-MPiper (Table 2). Consequently, the initial HYD selectivity, which was obtained by extrapolation to zero weight time, decreased in the presence of the amines from 65% to 44% and 42% at 1 kPa 2-MPy and 2-MPiper, respectively, and to 39% and 26% at 6 kPa of 2-MPy and 2-MPiper, respectively. This

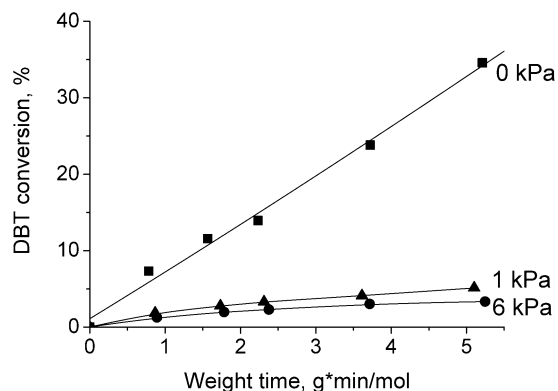


Fig. 1. Conversion of 1 kPa DBT in the absence and presence of 2-methylpyridine at 340 °C over Mo/γ-Al<sub>2</sub>O<sub>3</sub>.

Table 1  
HDS of 1 kPa DBT in the presence of 2-MPy at 340 °C over Mo/ $\gamma$ -Al<sub>2</sub>O<sub>3</sub> and CoMo/ $\gamma$ -Al<sub>2</sub>O<sub>3</sub> ( $\tau = 5$  g min/mol) and NiMo/ $\gamma$ -Al<sub>2</sub>O<sub>3</sub> ( $\tau = 3.5$  g min/mol)

Conversion (%)	Mo			CoMo				NiMo			
	0 kPa	1 kPa	6 kPa	0 kPa	1 kPa	2 kPa	6 kPa	0 kPa	2 kPa	6 kPa	10 kPa
Total	34.6	5.1	3.3	81.9	38.1	29.2	23.2	76.9	74.8	50.7	48.7
DDS	8.5	2.9	2.0	55.0	32.7	26.0	20.3	57.5	69.0	49.3	47.6
CHB	11.8	0.5	0.2	23.6	4.3	2.0	1.6	18.2	2.3	0.9	0.5
BCH	2.6	–	–	2.5	–	–	–	–	–	–	–
TH-DBT	9.0	1.4	1.0	0.7	1.0	1.0	1.1	1.2	0.5	0.5	0.6
HH-DBT	2.7	0.3	0.1	0.1	0.1	0.2	0.2	–	–	–	–

Table 2  
HDS of 1 kPa DBT in the presence of 2-MPiper at 340 °C over Mo/ $\gamma$ -Al<sub>2</sub>O<sub>3</sub> and CoMo/ $\gamma$ -Al<sub>2</sub>O<sub>3</sub> ( $\tau = 5$  g min/mol) and NiMo/ $\gamma$ -Al<sub>2</sub>O<sub>3</sub> ( $\tau = 3.5$  g min/mol)

Conversion (%)	Mo			CoMo				NiMo			
	0 kPa	1 kPa	6 kPa	0 kPa	1 kPa	2 kPa	6 kPa	0 kPa	2 kPa	6 kPa	10 kPa
Total	34.6	3.7	3.0	81.9	34.3	27.1	13.3	76.9	73.8	59.6	50.2
DDS	8.5	2.0	2.2	55.0	29.9	24.0	12.0	57.5	72.8	58.9	49.7
CHB	11.8	0.3	0.2	23.6	3.4	2.2	0.5	18.2	0.8	0.4	0.2
BCH	2.6	–	–	2.5	–	–	–	–	–	–	–
TH-DBT	9.0	1.2	0.5	0.7	0.9	0.7	0.7	1.2	0.2	0.3	0.3
HH-DBT	2.7	0.2	0.1	0.1	0.1	0.2	0.1	–	–	–	–

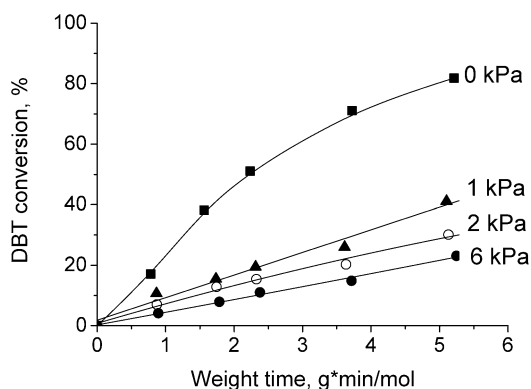


Fig. 2. Conversion of 1 kPa DBT in the absence and presence of 2-methylpyridine at 340 °C over CoMo/ $\gamma$ -Al<sub>2</sub>O<sub>3</sub>.

indicates that both amines have a strong inhibitory influence on the HDS of DBT, but the HYD pathway is suppressed more strongly than the DDS pathway. 2-MPiper inhibits the overall HDS and the HYD pathway slightly more strongly than 2-MPy (cf. Tables 1 and 2).

The conversion of 1 kPa DBT over CoMo/ $\gamma$ -Al<sub>2</sub>O<sub>3</sub> decreased by a factor of 2.1 at 1 kPa 2-MPy (Fig. 2) and by a factor of 2.4 at 1 kPa 2-MPiper (Table 2). An increase in the partial pressure of the amine to 2 and 6 kPa led to a further decrease in the conversion of DBT. Thus, at 6 kPa 2-MPy and 2-MPiper the overall conversion of DBT was suppressed by factors of 3.5 and 6.2, respectively. The HYD pathway was inhibited more strongly than the DDS pathway. At 1 kPa 2-MPy, HYD conversion was reduced by a factor of 5, and DDS conversion was decreased by a factor 1.7. The corresponding factors for 2-MPiper were 6.1 for HYD and 1.8 for DDS. Consequently, the initial HYD selectivity decreased from 30% to 14% and 11% at 1 kPa 2-MPy and 2-MPiper, 13% and 10% at 2 kPa 2-MPy and 2-MPiper, and 12% and 8% at 6 kPa 2-MPy and

2-MPiper, respectively. Thus, as for the Mo/ $\gamma$ -Al<sub>2</sub>O<sub>3</sub> catalyst, 2-MPiper suppressed the overall HDS and the HYD pathway more strongly than 2-MPy.

The influence of 2-MPy and 2-MPiper on the HDS of DBT at 340 °C over NiMo/ $\gamma$ -Al<sub>2</sub>O<sub>3</sub> was studied previously [9]. The results, given in Tables 1 and 2, show that both amines strongly suppressed the HYD pathway; at 2 kPa amine, 2-MPy reduced it by a factor 6.9 and 2-MPiper by a factor 19.4. The DDS pathway was not suppressed, but was promoted at low amine partial pressure. Only at high amine partial pressure was there a weak inhibition.

### 3.2. HDS of 4,6-DMDBT at 340 °C

The HDS of 4,6-DMDBT in the presence of 2-MPy and 2-MPiper was studied at 340 °C and 35 kPa H<sub>2</sub>S over Mo/ $\gamma$ -Al<sub>2</sub>O<sub>3</sub> and CoMo/ $\gamma$ -Al<sub>2</sub>O<sub>3</sub> catalysts. Over the Mo/ $\gamma$ -Al<sub>2</sub>O<sub>3</sub> catalyst, the reactivity of 1 kPa 4,6-DMDBT was strongly suppressed at 2 kPa 2-MPy and 2-MPiper (Fig. 3). The conversion of 4,6-DMDBT at  $\tau = 5$  g min/mol reached only 4.5% in the presence of 2-MPy and 2.5% in the presence of 2-MPiper (Tables 3 and 4). The initial HYD selectivity decreased from 84% in the absence to 82% in the presence of 2-MPy and 80% in the presence of 2-MPiper. Again, 2-MPiper inhibited the overall HDS and the HYD pathway more strongly than 2-MPy.

The activity of the CoMo/ $\gamma$ -Al<sub>2</sub>O<sub>3</sub> catalyst in the HDS of 4,6-DMDBT was even more strongly inhibited by 2 kPa 2-MPy and 2-MPiper than that of Mo/ $\gamma$ -Al<sub>2</sub>O<sub>3</sub> (Tables 3 and 4). The conversion of 4,6-DMDBT was only 3.4% in the presence of 2-MPy and 3% in the presence of 2-MPiper. Consequently, the performance of CoMo/ $\gamma$ -Al<sub>2</sub>O<sub>3</sub> in the presence of N-compounds was similarly low as that of the Mo/ $\gamma$ -Al<sub>2</sub>O<sub>3</sub> catalyst. The initial HYD selectivity decreased from 88% in the absence to 75% and 70% in the presence of 2-MPy and 2-

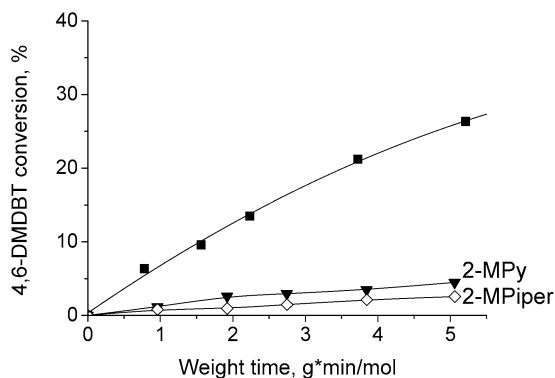


Fig. 3. Conversion of 1 kPa 4,6-DMDBT in the absence and presence of 2 kPa 2-methylpyridine and 2-methylpiperidine at 340 °C over Mo/γ-Al<sub>2</sub>O<sub>3</sub>.

Table 3

HDS of 1 kPa 4,6-DMDBT in the presence of 2-MPy over Mo/γ-Al<sub>2</sub>O<sub>3</sub>, CoMo/γ-Al<sub>2</sub>O<sub>3</sub>, and NiMo/γ-Al<sub>2</sub>O<sub>3</sub> at 340 °C and τ = 5 g min/mol

Conversion (%)	Mo		CoMo		NiMo		
	0 kPa	2 kPa	0 kPa	2 kPa	0 kPa	2 kPa	6 kPa
Total	26.3	4.5	49.1	3.4	46.4	12.4	3.3
DDS	4.1	0.8	5.4	0.9	11.7	4.3	1.4
MCHT	6.3	0.3	28.3	0.6	24.5	1.3	–
DMBCH	10.2	0.4	13.0	0.1	4.4	1.2	–
DM-TH-DBT	5.7	3.0	2.4	1.8	5.8	5.6	1.9

Table 4

HDS of 1 kPa 4,6-DMDBT in the presence of 2-MPiper over Mo/γ-Al<sub>2</sub>O<sub>3</sub>, CoMo/γ-Al<sub>2</sub>O<sub>3</sub>, and NiMo/γ-Al<sub>2</sub>O<sub>3</sub> at 340 °C and τ = 5 g min/mol

Conversion (%)	Mo		CoMo		NiMo		
	0 kPa	2 kPa	0 kPa	2 kPa	0 kPa	2 kPa	6 kPa
Total	26.3	2.5	49.1	3.0	46.4	11.5	2.5
DDS	4.1	0.5	5.4	0.9	11.7	4.2	1.1
MCHT	6.3	0.1	28.3	0.6	24.5	1.1	–
DMBCH	10.2	0.2	13.0	0.1	4.4	1.0	–
DM-TH-DBT	5.7	1.7	2.4	1.4	5.8	5.2	1.4

MPiper, respectively. Therefore, 2-MPiper inhibited the overall HDS and the HYD pathway more strongly than 2-MPy.

The influence of 2-MPy and 2-MPiper on the HDS of 4,6-DMDBT at 340 °C over NiMo/γ-Al<sub>2</sub>O<sub>3</sub> was studied previously [11]; the results are given in Tables 3 and 4. Both amines suppressed both HDS pathways, but the HYD pathway more strongly than the DDS pathway. Again, 2-MPiper had a stronger effect than 2-MPy.

### 3.3. The effect of N-compounds on the HDS of DBT at 300 °C

Previously we reported a promoting effect of low concentrations of 2-MPiper on the HDS of DBT over NiMo/γ-Al<sub>2</sub>O<sub>3</sub> [10]. To see whether such a promotion effect also occurred for CoMo/γ-Al<sub>2</sub>O<sub>3</sub> and Mo/γ-Al<sub>2</sub>O<sub>3</sub>, we investigated the HDS of DBT over these two catalysts at 300 °C and 0.1 kPa 2-MPiper; however, no promotional effect was observed. The overall conversion of DBT was suppressed by a factor of 1.7 at 0.1 kPa 2-MPiper over the CoMo/γ-Al<sub>2</sub>O<sub>3</sub> catalyst (Fig. 4). HYD conversion decreased from 11% to 2%, and DDS con-

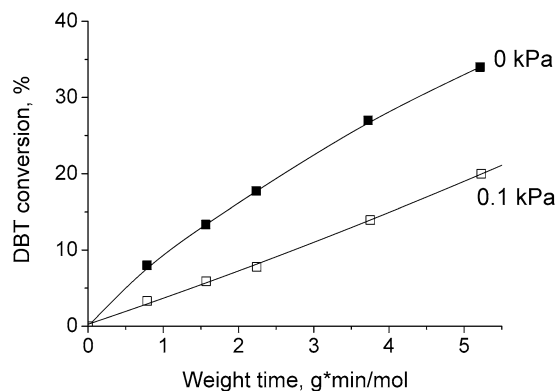


Fig. 4. Conversion of 1 kPa DBT in the absence and presence of 2-methylpiperidine at 300 °C over CoMo/γ-Al<sub>2</sub>O<sub>3</sub>.

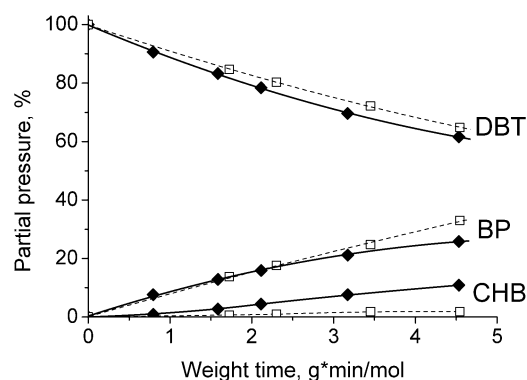


Fig. 5. HDS of 1 kPa DBT in the absence (◆) and presence (□) of 0.1 kPa neopentylamine at 300 °C over NiMo/γ-Al<sub>2</sub>O<sub>3</sub>.

version decreased from 23% to 18%. Thus, HYD selectivity decreased from 32% to 10%, demonstrating that not only at 340 °C (Section 3.1), but also at 300 °C, the inhibitory influence was much more pronounced for the HYD pathway over the CoMo catalyst. Similarly, no promoting effect was observed for the HDS of DBT over the Mo catalyst, or for the HDS of 4,6-DMDBT over the NiMo catalyst. The promotion effect seems to be unique for the combination NiMo and DBT.

To examine the influence of the amine in the HDS of DBT in the presence of the NiMo catalyst, we tested several amines (neopentylamine, dipropylamine, piperidine, 2-methylpyrrolidine, and N,N-dimethylaniline) in addition to the two amines (2-MPiper and 2-MPy) that we had studied in previous work [10]. Neopentylamine was chosen because it is a primary amine, whereas dipropylamine, piperidine, and 2-methylpyrrolidine are secondary amines (which are more basic than primary amines) with noncyclic and cyclic structures. In addition to the aromatic 2-methylpyridine, which we had studied in previous work, we chose N,N-dimethylaniline. All amines, with the exception of dipropylamine, underwent hydrodenitrogenation only very slowly at 300 °C and thus remained present during the entire HDS reaction of DBT. All experiments were performed as before [10] at 300 °C and 35 kPa H<sub>2</sub>S.

In the presence of 0.1 kPa neopentylamine, the conversion of DBT decreased slightly, but the formation of biphenyl was enhanced (Fig. 5 and Table 5). The HYD pathway was



Table 5  
HDS results and DDS ( $k_{\text{DDS}}$ ) and HYD ( $k_{\text{HYD}}$ ) rate constants (in  $10^{-2} \text{ mol g}^{-1} \text{ min}^{-1}$ ) of 1 kPa DBT in the presence of 0.1 kPa amine over NiMo/ $\gamma$ -Al<sub>2</sub>O<sub>3</sub> at 300 °C and  $\tau = 4.5 \text{ g min/mol}$

Conversion (%)	$100 \times k$ (mol g <sup>-1</sup> min <sup>-1</sup> )	0 kPa	NPA	DPA	N,N-DMA	2-MPy	Piper	2-MPiper	2-MPyrrolid
Total		38.4	35.9	36.2	36.5	37.6	42.9	44.4	44.7
DDS		25.9	33.0	30.2	28.2	35.3	40.0	42.2	41.5
CHB		10.9	1.9	4.5	6.1	1.5	2.1	1.5	2.6
TH-DBT		1.6	1.0	1.5	2.2	0.7	0.6	0.7	0.6
	$k_{\text{DDS}}$	9.2	8.7	9.3	9.1	11.1	12.2	12.8	12.5
	$k_{\text{HYD}}$	1.8	1.0	0.8	1.1	0.4	0.6	0.4	0.4

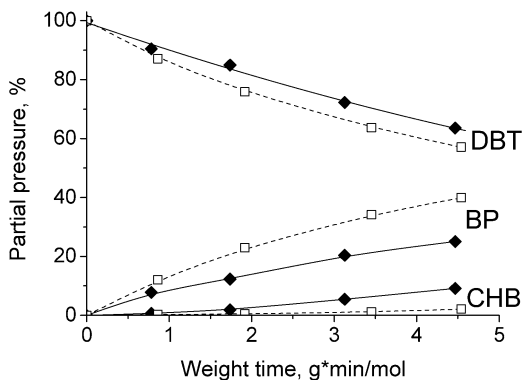


Fig. 6. HDS of 1 kPa DBT in the absence (◆) and presence (□) of 0.1 kPa piperidine at 300 °C over NiMo/ $\gamma$ -Al<sub>2</sub>O<sub>3</sub>.

strongly suppressed, because the amount of cyclohexylbenzene formed was five times lower than in the absence of neopentylamine. The amount of tetrahydrodibenzothiophene, the intermediate in the HYD pathway, was only slightly lower. This indicates that not only the hydrogenation reaction, but also the further desulfurization reaction in the HYD pathway, was suppressed. Also, dipropylamine and N,N-dimethylaniline slightly inhibited the HDS of DBT (Table 5). Again, this inhibition was due to suppression of the HYD pathway, whereas the formation of biphenyl was enhanced. 2-Methylpyridine behaved similarly (Table 5), as described previously [10].

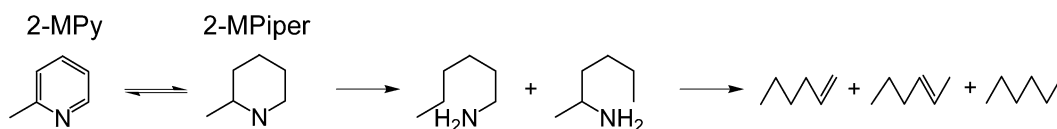
In the presence of 0.1 kPa piperidine, the conversion of DBT was enhanced by 4.5% at the highest weight time (Fig. 6). This increase was due to a strong promotion of the DDS pathway (Table 5), as was observed previously for 2-methylpiperidine [10]. The initial HYD selectivity decreased from 15% to 5%. The HYD pathway was strongly suppressed, as in all competitive experiments, and the yield of cyclohexylbenzene decreased by a factor of five. The yield of the partially hydrogenated intermediate tetrahydrodibenzothiophene was lower in the presence of amine. The effect of 2-methylpyrrolidine was very similar to that of piperidine and 2-methyl-

piperidine. DBT conversion and biphenyl formation were enhanced in the presence of 0.1 kPa 2-methylpyrrolidine, whereas the amounts of cyclohexylbenzene and partially hydrogenated intermediate decreased (Table 5).

### 3.4. HDN of 2-MPy and 2-MPiper over Mo/ $\gamma$ -Al<sub>2</sub>O<sub>3</sub> and CoMo/ $\gamma$ -Al<sub>2</sub>O<sub>3</sub>

To further compare the hydrogenation properties of the NiMo, CoMo, and Mo catalysts, we studied the HDN of 2-MPy and 2-MPiper at 340 °C and 35 kPa H<sub>2</sub>S. The HDN of 2-MPy occurs via hydrogenation to 2-MPiper and breaking of the resulting aliphatic C–N bond with the formation of hexylamine and 2-aminohexane, which are further converted to hexenes and hexane (Scheme 1) [12]. The most abundant products of the HDN of 2-MPy over CoMo/ $\gamma$ -Al<sub>2</sub>O<sub>3</sub> were 2-MPiper, 1-hexene and 2-hexene (which we denote as hexenes in what follows), and hexane, the final product (Fig. 7). Hexylamine and 2-aminohexane were observed in very small amounts, indicating that cleavage of the second C–N bond is easy. 2-Methyl-3,4,5,6-tetrahydropyridine (2-methylpiperidine-imine) was also present in small amounts.

The conversion of 2-MPy was higher over the Mo/ $\gamma$ -Al<sub>2</sub>O<sub>3</sub> catalyst than over the CoMo/ $\gamma$ -Al<sub>2</sub>O<sub>3</sub> catalyst (cf. Figs. 7 and 8), but this was due mainly to the rapid hydrogenation to 2-MPiper. The subsequent nitrogen removal reactions were slower over the Mo/ $\gamma$ -Al<sub>2</sub>O<sub>3</sub> catalyst than over the Co-promoted catalyst. The yield of C<sub>6</sub> products hardly reached 4% at  $\tau = 5 \text{ g min/mol}$ , whereas it was four times higher over CoMo/ $\gamma$ -Al<sub>2</sub>O<sub>3</sub> (Figs. 7 and 8). The hexylamine, 2-aminohexane, and 2-methyl-3,4,5,6-tetrahydropyridine (2-methylpiperidine-imine) intermediates were detected in more pronounced amounts than over the promoted catalyst. Thus, despite its good hydrogenation performance, the degree of denitrogenation over Mo/ $\gamma$ -Al<sub>2</sub>O<sub>3</sub> is low. The conversion of 2-MPy over CoMo/ $\gamma$ -Al<sub>2</sub>O<sub>3</sub> was almost equal to that over NiMo/ $\gamma$ -Al<sub>2</sub>O<sub>3</sub> [12], but the yield of C<sub>6</sub> products was higher over the CoMo catalyst (Table 6).



Scheme 1. Reaction network of the HDN of 2-methylpyridine and 2-methylpiperidine.

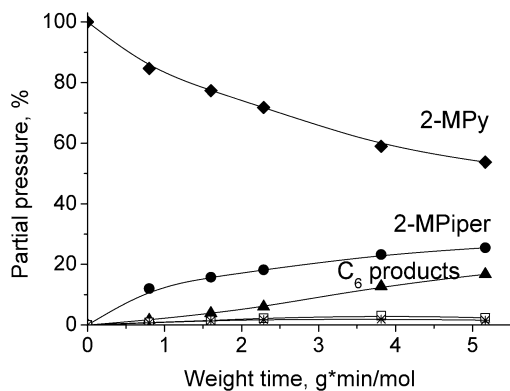


Fig. 7. HDN of 2-methylpyridine over  $\text{CoMo}/\gamma\text{-Al}_2\text{O}_3$  at  $340^\circ\text{C}$  (◆, 2-methylpyridine; ●, 2-methylpiperidine; ▲, hexenes and hexane; □, hexylamine and 2-aminohexane; \*, 2-methyl-3,4,5,6-tetrahydropyridine).

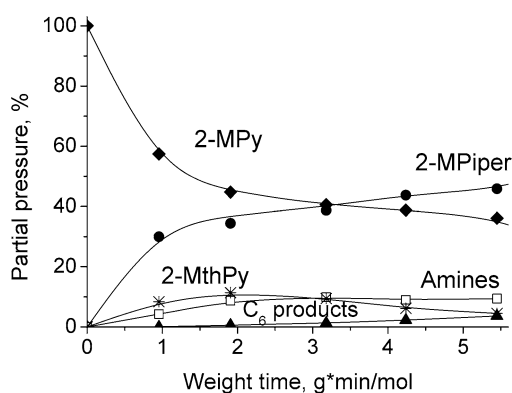


Fig. 8. HDN of 2-methylpyridine over  $\text{Mo}/\gamma\text{-Al}_2\text{O}_3$  at  $340^\circ\text{C}$  (◆, 2-methylpyridine; ●, 2-methylpiperidine; ▲, hexenes and hexane; □, hexylamine and 2-aminohexane; \*, 2-methyl-3,4,5,6-tetrahydropyridine).

Table 6

HDN of 2-methylpyridine over  $\text{Mo}/\gamma\text{-Al}_2\text{O}_3$ ,  $\text{CoMo}/\gamma\text{-Al}_2\text{O}_3$ , and  $\text{NiMo}/\gamma\text{-Al}_2\text{O}_3$  at  $340^\circ\text{C}$  and  $\tau = 5$  g min/mol

Yields (%)	Mo	CoMo	NiMo
Conversion	62.8	46.2	47.0
2-MPiper	45.2	25.5	34.2
C <sub>6</sub> -products	3.1	16.7	10.9
Amines	9.5	2.4	1.4
2-MTHPy	5.0	1.6	0.5

The HDN of 2-MPiper over  $\text{CoMo}/\gamma\text{-Al}_2\text{O}_3$  showed that 2-MPiper quickly converts to 2-methyl-3,4,5,6-tetrahydropyridine, 2-MPy, and hexylamines (Fig. 9). Above  $\tau = 3$  g min/mol, the C<sub>6</sub> products became the most abundant products. The 2-MPiper conversion, yield of hexenes and hexane, and yield of hexylamines at  $\tau = 5$  g min/mol were 65, 32, and 18% over the CoMo catalyst (Fig. 9) and 33, 22, and 4.5% over the NiMo catalyst [12], respectively. But comparing these data is difficult, because the conversion of 2-MPiper over the CoMo and NiMo catalysts differed by a factor of two. Therefore, it makes more sense to compare the yields obtained at  $\tau = 3.8$  g min/mol for CoMo and  $\tau = 8.8$  g min/mol for NiMo, where a similar conversion of 57% was achieved. The yields of C<sub>6</sub> products and hexylamines were 25 and 16% over CoMo and 41 and 4.5%

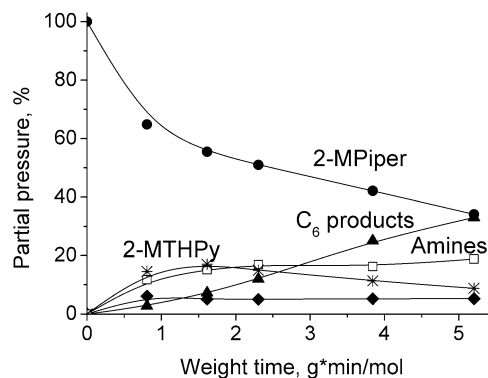


Fig. 9. HDN of 2-methylpiperidine over  $\text{CoMo}/\gamma\text{-Al}_2\text{O}_3$  at  $340^\circ\text{C}$  (●, 2-methylpiperidine; ▲, hexenes and hexane; □, hexylamine and 2-aminohexane; \*, 2-methyl-3,4,5,6-tetrahydropyridine; ◆, 2-methylpyridine).

over NiMo, respectively. These results show that the cleavage of the first C–N bond was easier over the Co-promoted catalyst, whereas the cleavage of the second C–N bond was easier over the Ni-promoted catalyst.

## 4. Discussion

### 4.1. HYD and DDS rate constants

Our results show that amines influence the DDS and HYD pathways differently, in accordance with previously reported findings [2,5–8]. The inhibition was stronger for the HYD pathway than for the DDS pathway for all three  $\gamma\text{-Al}_2\text{O}_3$ -supported catalysts NiMo, CoMo, and Mo (Table 1). When a molecule reacts by two parallel reactions that are influenced differently by an additive, a change in the conversion along one pathway does not automatically mean that the corresponding rate constant changes in proportion to this change. In our case, suppression of the HYD pathway by the amines means that more DBT is available for the DDS pathway. This leads to a higher DDS conversion, even if the rate constant,  $k_{\text{DDS}}$ , does not change. In addition, the conversion of biphenyl (the product of the DDS pathway) to cyclohexylbenzene (the product of the HYD pathway) is lower, because the amines suppress the hydrogenation not only of DBT, but also of biphenyl. These factors were taken into account in a first-order analysis of the conversions and initial selectivities. The resulting rate constants,  $k_{\text{DDS}}$  for the DDS pathway and  $k_{\text{HYD}}$  for the HYD pathway, show that methyl groups in the 4 and 6 positions of 4,6-DMDBT, close to the sulfur atom, had a minor positive effect on  $k_{\text{HYD}}$  over Mo and CoMo but noticeably increased  $k_{\text{HYD}}$  over NiMo (Table 7). On the other hand, methyl groups decreased  $k_{\text{DDS}}$  by more than a factor of 10 for the CoMo and NiMo catalysts and by a factor of 3 for the Mo catalyst. As proposed previously [13], this suggests that when 4,6-DMDBT adsorbs on a hydrogenation site, the methyl groups do not point toward the surface, whereas when 4,6-DMDBT is adsorbed on a DDS site, the methyl groups do point towards the surface. In agreement with this suggestion, amines and  $\text{H}_2\text{S}$  affected the DDS and HYD reactions differently; 2-MPy decreased the  $k_{\text{HYD}}$  constants more than the  $k_{\text{DDS}}$  constants (Table 7) and  $\text{H}_2\text{S}$  decreased  $k_{\text{DDS}}$  more

Table 7

DDS ( $k_{\text{DDS}}$ ) and HYD ( $k_{\text{HYD}}$ ) rate constants (in  $10^{-2} \text{ mol g}^{-1} \text{ min}^{-1}$ ) of DBT and 4,6-DMDBT in the absence and presence of 2 kPa 2-methylpyridine over Mo/ $\gamma$ -Al<sub>2</sub>O<sub>3</sub>, CoMo/ $\gamma$ -Al<sub>2</sub>O<sub>3</sub>, and NiMo/ $\gamma$ -Al<sub>2</sub>O<sub>3</sub> at 340 °C, 5 MPa, 35 kPa H<sub>2</sub>S

Catalyst	2-MPy (kPa)	DBT		4,6-DMDBT	
		$k_{\text{DDS}}$	$k_{\text{HYD}}$	$k_{\text{DDS}}$	$k_{\text{HYD}}$
Mo	0	2.7	5	1	5.1
	2	0.6 <sup>a</sup>	0.5 <sup>a</sup>	0.2	0.8
CoMo	0	26	11	1.7	13
	2	5.9	0.8	0.2	0.5
NiMo	0	35	3.9	2.9	9
	2	34	1.4	1.0	1.8

<sup>a</sup> Data measured at 1 kPa 2-MPy.

strongly than  $k_{\text{HYD}}$  for DBT and 4,6-DMDBT over all three catalysts [14]. Other groups obtained similar results [13,15–19]. Therefore, the effect of H<sub>2</sub>S (weak acid) is opposite to that of the amines (bases), which points to an acid–base interaction of adsorbate and catalytic site. Apparently, the HYD sites have a more acidic character, and the DDS sites have a more basic character [15].

Whereas  $k_{\text{HYD}}$  of the HDS of DBT and 4,6-DMDBT over all three catalysts and  $k_{\text{DDS}}$  over CoMo and Mo decreased from the addition of small amounts of amine,  $k_{\text{DDS}}$  of the HDS of DBT over NiMo was hardly affected or increased (Tables 5 and 7). Thus, at 300 °C,  $k_{\text{HYD}}$  decreased from 0.018 mol/(g min) in the absence of amine to 0.008–0.011 mol/(g min) in the presence of 0.1 kPa neopentylamine, dipropylamine, and N,N-dimethylaniline and to 0.004–0.006 mol/(g min) in the presence of 0.1 kPa 2-methylpyridine, piperidine, 2-methylpiperidine, and 2-methylpyrrolidine (Table 5). In contrast, within the uncertainty of measurements, the DDS rate constant remained equal to 0.09 mol/(g min), the value in the absence of amine, when 0.1 kPa neopentylamine, dipropylamine, and N,N-dimethylaniline were present. In the presence of 2-methylpyridine, piperidine, 2-methylpiperidine, and 2-methylpyrrolidine, however, the DDS rate constant increased to 0.11–0.13 mol/(g min). Thus, the cyclic amines behaved differently in the HDS of DBT over NiMo/ $\gamma$ -Al<sub>2</sub>O<sub>3</sub> at low concentration. They inhibited the HYD pathway like all other amines, but promoted the DDS pathway so much that the total HDS conversion was higher than that in the absence of amine. We believe that the special effect of the cyclic amines is due to the fact that they have a higher basicity than the other amines. Only dipropylamine has a similarly high basicity, but in contrast to the cyclic amines, it is not stable under reaction conditions. Dialkylamines are quickly converted to alkylamines and alkanethiols [20], and the alkylamines (cf. neopentylamine) do not promote the DDS pathway. 2-Methylpyridine had a similar effect on the HDS of DBT as cyclic amines (Table 5), although only a weak promotion of the DBT conversion was observed. This is explained by the rapid transformation of 2-methylpyridine to 2-methylpiperidine under the reaction conditions. Thus, the inhibiting action of 2-methylpyridine was compensated for by the promoting action of 2-methylpiperidine.

## 4.2. Catalyst surface

To explain the general inhibition of amines on the HYD pathway and the special promotion of cyclic amines, exclusively in the HDS of DBT over NiMo/ $\gamma$ -Al<sub>2</sub>O<sub>3</sub>, we first consider what makes the catalyst surface of NiMo/ $\gamma$ -Al<sub>2</sub>O<sub>3</sub> so special and why DBT behaves differently than 4,6-DMDBT. It is generally assumed that the catalytically active sites in a Mo/ $\gamma$ -Al<sub>2</sub>O<sub>3</sub> hydrotreating catalyst are the molybdenum atoms at the edges and corners of the MoS<sub>2</sub> crystallites, which have at least one sulfur vacancy on the molybdenum atom and thus allow chemical adsorption of the reacting molecule [21–23]. Density functional theory (DFT) calculations indicate that under our HDS conditions (35 kPa H<sub>2</sub>S and 5 MPa H<sub>2</sub>), the Mo catalyst contains 50% sulfided Mo edges, with sulfur atoms in bridge positions between Mo atoms [24–29]. The Mo atoms at the Mo edge are thus fully coordinated by six sulfur atoms in a trigonal prismatic arrangement (Fig. 10). The most stable position for the Co or Ni promoter atom is at the edges of the MoS<sub>2</sub> particles, substituting a molybdenum atom [26] and forming the so-called Co–Mo–S and Ni–Mo–S structures [23]. The NiMo catalyst contains Ni atoms at the metal edge that are not covered by sulfur atoms and have a square-planar sulfur coordination with open coordination positions [26,28,29]. The Co atoms in the CoMo catalyst are preferentially situated at the sulfur edges [24,26,28,29]. DFT calculations indicate that the Mo atoms at the sulfur edges of MoS<sub>2</sub> [27–29] and Ni-promoted MoS<sub>2</sub>, as well as the Co atoms at the sulfur edges of Co-promoted MoS<sub>2</sub> [28,29] are 50% sulfided under normal HDS conditions. The Mo and Co atoms are surrounded by four sulfur atoms, the outer two of which are in bridge positions between the metal atoms. The bridge positions of the sulfur atoms on the Co atoms are regular, leading to a tetrahedral sulfur coordination around the Co atoms. In contrast, the bridging sulfur atoms on the Mo atoms have a zigzag configuration, so that four sulfur atoms in a distorted tetrahedron coordinate the Mo atoms. Fig. 10 shows the structures of the metal and sulfur edges of MoS<sub>2</sub>, Ni–MoS<sub>2</sub>, and Co–MoS<sub>2</sub> under normal HDS conditions.

## 4.3. DDS rate constants

The rate constants for the DDS of DBT in the absence of H<sub>2</sub>S are much larger than the hydrogenation rate constants and follow the order Mo  $\ll$  CoMo < NiMo [14]. Methyl groups in the 4 and 6 positions and H<sub>2</sub>S decrease these rate constants more than an order of magnitude, so that  $k_{\text{DDS}}$  of the HDS of 4,6-DMDBT becomes even smaller than  $k_{\text{HYD}}$  for all three catalysts (Table 7). The strong influence of the methyl groups and of H<sub>2</sub>S is easily explained by hindering of the  $\sigma$  adsorption on sulfur vacancies. The much lower  $k_{\text{DDS}}$  for Mo than for CoMo and NiMo can be explained by the locations and coverages of the Mo, Co, and Ni atoms. In Section 4.2 it was shown that the Mo atoms on the metal edge in the most stable MoS<sub>2</sub> structure are fully coordinated by six sulfur atoms and cannot adsorb DBT [24–29]. The removal of sulfur atoms from this fully covered Mo edge to create vacancies is very difficult [24,25,27,30,31], although one DFT calculation indicated that a low concentra-

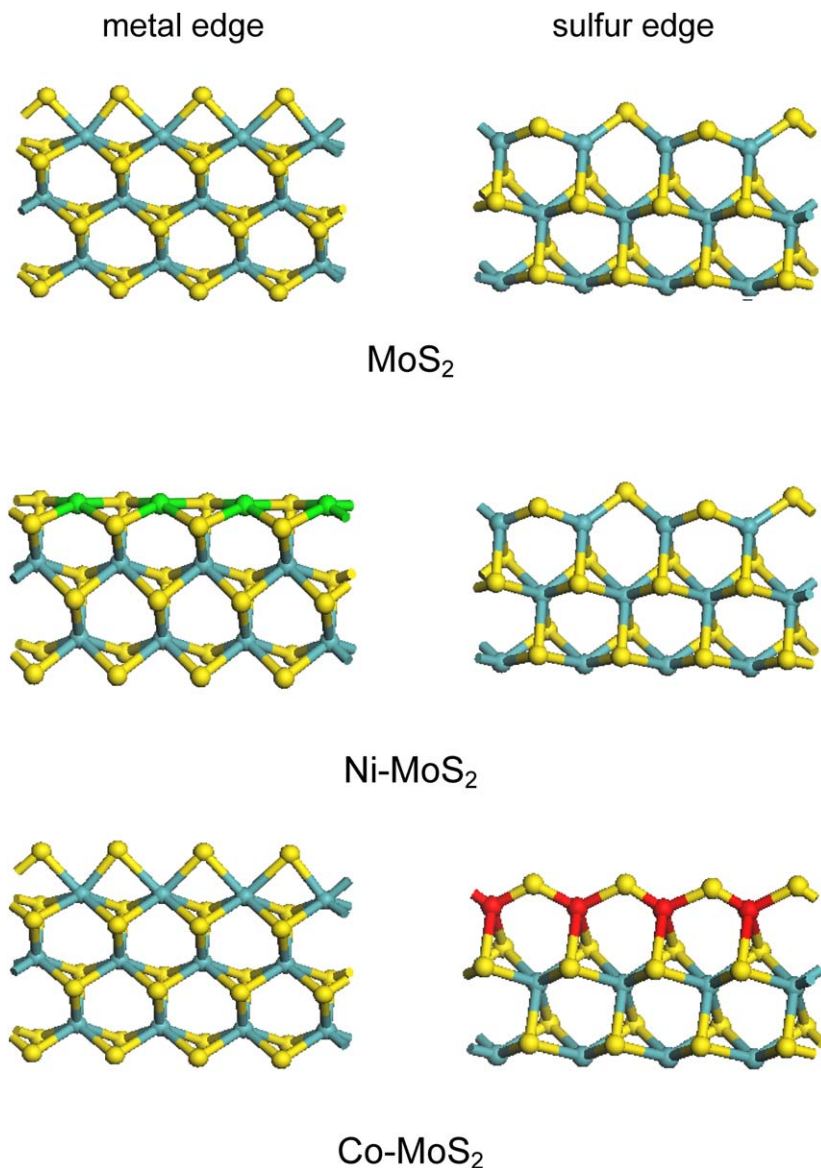


Fig. 10. Structure of the metal and sulfur edges of MoS<sub>2</sub>, Ni-MoS<sub>2</sub>, and Co-MoS<sub>2</sub> under normal HDS conditions as predicted by DFT calculations [24–29]. The sulfur atoms are in yellow, the Mo atoms in blue, the Ni atoms in green, and the Co atoms in red.

tion of vacancies may exist [32]. Cristol et al. showed that DBT molecules can adsorb in  $\eta^1$  ( $\sigma$ ) mode on such vacancies, but 4,6-DMDBT molecules cannot [33]. The relatively low DDS activity of the Mo catalyst may be due to these few sulfur vacancies on the Mo edges. The Mo atoms on the most stable sulfur edge of MoS<sub>2</sub> might also explain the low DDS activity. These Mo atoms have a distorted tetrahedral coordination (Fig. 10) [27–29], which would allow  $\eta^1$  adsorption of the incoming DBT molecules after rearrangement of the two external S atoms [33]. However, the Mo atoms on the sulfur edge have a formal charge of +0.67 and most likely bind H<sub>2</sub>S molecules strongly. As a result, the Mo atoms on the sulfur edge actually would not be coordinated by four sulfur atoms under normal HDS conditions, but rather by four sulfur atoms and one or two additional H<sub>2</sub>S molecules. Whereas most DFT calculations have only considered the thermodynamics of the dissociation of H<sub>2</sub>S on the catalyst surface into a sulfur atom and H<sub>2</sub>, one

calculation considered H<sub>2</sub>S adsorption and demonstrated that it is reasonably strong (80 kJ/mol) on the Ni atoms at the metal edge of the NiMo catalyst [32]. The fact that Mo–S bonding is stronger than Ni–S bonding suggests that H<sub>2</sub>S adsorption on the Mo atoms at the sulfur edge of the Mo catalyst may be substantial; consequently, the Mo atoms on both the metal edge and the sulfur edge would be totally covered. This would explain the low DDS activity of the Mo catalyst. The fact that the Mo catalyst has some activity (albeit very low) for the DDS of 4,6-DMDBT might be due to the existence of some special sites.

The higher DDS activity of the CoMo catalyst compared with that of the Mo catalyst may be explained by the weaker Co–S bond compared with the Mo–S bond, which will give a lower H<sub>2</sub>S adsorption on the sulfur edge of the CoMo catalyst. Thus, a higher number of sulfur vacancies will be present on the surface of the CoMo catalyst than on the surface of the Mo catalyst. The Ni atoms on the metal edge of the NiMo catalyst



have a square-planar sulfur coordination and one free coordination site (Fig. 10) [26,28,29]. Thus, they can easily adsorb DBT in the  $\sigma$  mode and induce a rapid DDS reaction. This explains why NiMo has the highest  $k_{\text{DDS}}$ .

#### 4.4. HYD rate constants

The HYD rate constant  $k_{\text{HYD}}$  is only moderately influenced by the methyl groups,  $\text{H}_2\text{S}$ , and the catalyst (Table 7). The methyl groups even have a positive influence, which must be due to the higher basicity of 4,6-DMDBT, and thus stronger  $\pi$  adsorption and faster hydrogenation. The weak influence of  $\text{H}_2\text{S}$  indicates that sulfur vacancies are not a prerequisite for hydrogenation. The moderate influence of the catalyst suggests that hydrogenation takes place on all edges of the Mo, CoMo, and NiMo catalysts, sulfur covered or not. The slightly stronger inhibition of the hydrogenation of DBT and 4,6-DMDBT over NiMo by  $\text{H}_2\text{S}$  may be due to hydrogenation on the almost sulfur-free nickel-covered metal edge, whereas hydrogenation is slower on the sulfur-covered metal edges of the CoMo and Mo catalysts. The AFM results of Lauritsen et al. are in good agreement with these findings; those authors observed that the so-called “brim sites” of the  $\text{MoS}_2$  particles (the Mo atoms just behind the edges) have a metallic character on the metal as well as on the sulfur edges [34]. This would explain why both edges are active in hydrogenation.

In contrast to  $\text{H}_2\text{S}$ , amines inhibit the hydrogenation of DBT and 4,6-DMDBT more strongly than their direct desulfurization (Table 7) and influence the NiMo and CoMo catalysts differently (Fig. 11 and Table 7). This is in agreement with a different position for the promoter atoms. Thus, 2-MPy and 2-MPiper inhibit the HDS of DBT and 4,6-DMDBT over the Mo and CoMo catalysts (Tables 1–4), and 2-MPiper has a stronger effect than 2-MPy. The NiMo catalyst is slightly less sensitive to the amines than the CoMo and Mo catalysts in the HDS of 4,6-DMDBT [11] (Fig. 11b) and much less sensitive in the HDS of DBT [9] (Fig. 11a). At low concentrations, cyclic amines even promote the HDS of DBT over NiMo/ $\gamma$ - $\text{Al}_2\text{O}_3$ .

The differences between the NiMo/ $\gamma$ - $\text{Al}_2\text{O}_3$  catalyst on the one hand and the CoMo/ $\gamma$ - $\text{Al}_2\text{O}_3$  and Mo/ $\gamma$ - $\text{Al}_2\text{O}_3$  catalysts on the other hand must be due to the differences in the locations of the metal atoms on the metal and sulfur edges of the  $\text{MoS}_2$  crys-

tallites. Amines are basic and will adsorb on acid sites on the catalyst surface. These are SH groups on the sulfur and metal edges and exposed metal atoms on the metal edge. As shown in Fig. 10, the metal edges of the Mo and CoMo catalysts contain Mo atoms that are fully coordinated by basic S atoms and acidic SH groups are not present. The Mo and Co atoms on the sulfur edges of the Mo and CoMo catalysts, respectively, are tetrahedrally coordinated by S atoms and most likely further coordinated by  $\text{H}_2\text{S}$  molecules, as discussed above. The  $\text{H}_2\text{S}$  molecules combine with the S atoms to SH groups. Amines can adsorb on the SH groups and prohibit adsorption of DBT and 4,6-DMDBT and thus also prohibit their hydrogenation. The sulfur edge of the NiMo catalyst has the same structure as that of the Mo catalyst. The Ni sites at the metal edge of the NiMo catalyst are hardly covered by SH groups, which can adsorb amine molecules.

This unusual resistance of the Ni-promoted catalyst has been explained by a geometrical effect [10]. When 2-MPiper adsorbs in the  $\sigma$  mode on a Ni or Mo atom at the metal edge, it leaves the neighboring metal atom free. A single metal atom is not sufficient for the  $\pi$  adsorption and hydrogenation of DBT, but can adsorb DBT in the  $\sigma$  mode. In this way, at low amine partial pressure, HYD sites, which consist of several adjacent sulfur-free metal atoms, are transformed into DDS sites [10]. Thus, low amine concentrations even promote the HDS of DBT, but suppress the HDS of 4,6-DMDBT. At higher partial pressure, the amine molecules block many metal centers on the metal edge and also decrease the rate of the DDS pathway.

In discussing the DDS and HYD pathways, we have assumed that these two pathways occur independently and that  $\sigma$  and  $\pi$  adsorption of DBT or 4,6-DMDBT determine HDS selectivity. Although most of the literature agrees with these assumptions, as early as 1981 Singhal et al. proposed that the DDS and HYD pathways have a dihydro-DBT intermediate in common [35]. Recently, Bataille et al. [36] and Mi-join et al. [37] repeated this proposal and considered Hofmann elimination to be exclusively responsible for the C–S bond breakage. They explained the DDS and HYD selectivity by further reactions of the dihydro intermediate (i.e., direct elimination or further hydrogenation, followed by elimination), not by the adsorption of the DBT and 4,6-DMDBT molecules. In doing so, they had to assume that the DDS reaction

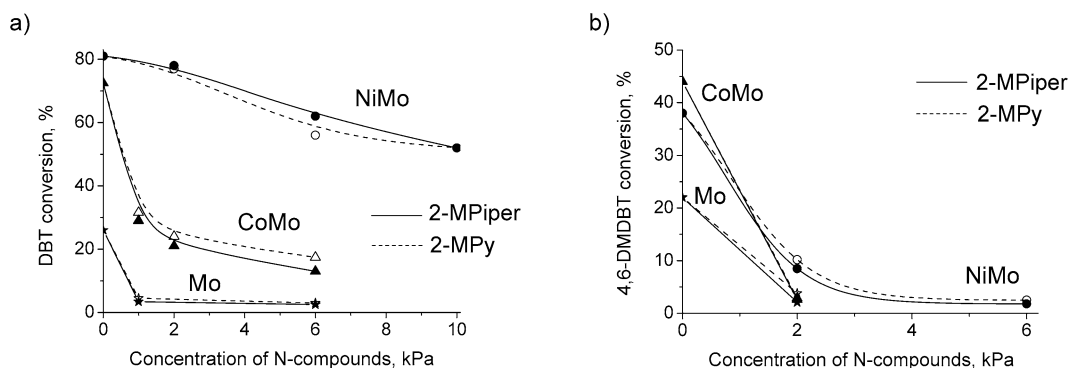


Fig. 11. Conversion of DBT (a) and 4,6-DMDBT (b) in the presence of 2-methylpyridine and 2-methylpiperidine over NiMo/ $\gamma$ - $\text{Al}_2\text{O}_3$ , CoMo/ $\gamma$ - $\text{Al}_2\text{O}_3$ , and Mo/ $\gamma$ - $\text{Al}_2\text{O}_3$  at  $\tau = 4$  g min/mol.

occurs through the 4,6-DM-4,4a-dihydro-DBT and 4,6-DM-4a,9b-dihydro-DBT intermediates, which are the only dihydro intermediates that can undergo DDS by elimination [36], even though they are kinetically as well as thermodynamically the least likely dihydro intermediates. No mention was made of the fact that methanethiol reacts very quickly to methane and H<sub>2</sub>S over metal sulfide catalysts. Elimination cannot explain this sulfur removal but hydrogenolysis can, as DFT calculations have shown [38]. Even alkanethiols that can undergo elimination still react by hydrogenolysis as well. Thus, Kieran and Kemball showed as early as 1965 that ethanethiol reacts to ethene and ethane in approximately equal amounts [39], and, more recently, it was shown that the alkane/alkene ratio in the HDS of alkanethiols depends strongly on pressure and the H<sub>2</sub>S/H<sub>2</sub> ratio [20]. Therefore, there is no reason to discount the mode of adsorption of the reacting molecules on the catalyst surface as the determining factor in the HDS of DBT and 4,6-DMDBT.

#### 4.5. HDN

The differences between the Mo, CoMo, and NiMo catalysts are also apparent in the HDN of 2-MPy. As shown by Scheme 1, the HDN reaction of 2-MPy is composed of a sequence of reactions. 2-MPy is first hydrogenated to 2-MPiper, after which C–N bond breaking occurs, first to hexylamine or 2-aminohexane and then to hexane and hexenes and ammonia [12]. The conversion of 2-MPy is determined solely by the rate of hydrogenation of 2-MPy to 2-MPiper, but the degree of nitrogen removal (i.e., yield of C<sub>6</sub> and C<sub>6</sub><sup>≡</sup>) is determined by the rate of C–N bond breaking as well. At  $\tau = 5$  g min/mol, Mo had the highest conversion of 2-MPy but the lowest degree of nitrogen removal (Figs. 7 and 8, Table 6). In fact, the yield of C<sub>6</sub> products formed over Mo was lower than that of hexylamines, indicating that the Mo catalyst had difficulty cleaving both the first and second C–N bonds. The conversion of 2-MPy was about the same over the NiMo and CoMo catalysts (Table 6), but the breaking of the C–N bond was faster over CoMo, as demonstrated by the lower yield of 2-MPiper and the higher yield of C<sub>6</sub> products.

The lower conversion of 2-MPy for the CoMo and NiMo catalysts than for the Mo catalyst seems surprising, because the former catalysts are generally considered the better hydrogenation catalysts. Our results for the hydrogenation of DBT and 4,6-DMDBT confirmed this finding (Table 7), although the advantage of CoMo over Mo was only a factor of two in  $k_{\text{HYD}}$ , and NiMo performed similar to Mo in the HYD of DBT. The conversion of 2-MPy over the Mo catalyst at 340 °C was relatively fast in the beginning and then slowed down (Fig. 8). This points to product inhibition. A very strong inhibition by the 2-MPiper product was seen over the NiMo catalyst at 300 °C. Adding 1 kPa 2-MPiper decreased the initial reaction rate of 6 kPa 2-MPy by a factor of 6.9 [9]. Assuming Langmuir–Hinshelwood kinetics, this means that the adsorption constant for 2-MPiper is 35 times larger than that for 2-MPy. Although product inhibition will be less strong at 340 °C than at 300 °C, it will still be substantial. The lower conversion of 2-MPy over CoMo and NiMo than over Mo thus may be caused by stronger

product inhibition rather than by a lower hydrogenation rate constant.

The degree of denitrogenation (i.e., yield of hexane and hexenes) in the HDN of 2-MPy was much lower over Mo than over CoMo and NiMo, even though more 2-MPiper was produced (Table 6). The degree of denitrogenation was higher over CoMo than over NiMo at the same conversion of 2-MPy. This means that the rate of breaking of the first C–N bond followed the order CoMo > NiMo > Mo. However, in the HDN of 2-MPiper, at the same conversion, NiMo had a higher yield of C<sub>6</sub> products than CoMo, meaning that the cleavage of the second C–N bond followed the order NiMo > CoMo > Mo. Thus, despite faster breaking of the second C–N bond over the NiMo catalyst, the overall HDN conversion was higher over the CoMo catalyst. Zhao et al. showed that C–N bond breaking occurs through substitution of the alkylamine by a thiol group by reaction of the amine with H<sub>2</sub>S [20]. This substitution occurs not by a normal organic S<sub>N</sub>2 substitution reaction, but rather by dehydrogenation of the amine to an imine cation, followed by addition of H<sub>2</sub>S, elimination of NH<sub>3</sub>, and hydrogenation to the thiol [40].

#### 5. Conclusion

For molecules like 4,6-DMDBT, with alkyl groups close to the sulfur atom,  $\sigma$  adsorption and thus the contribution of the fast DDS pathway to HDS is strongly hindered. Consequently, deep HDS (removal of the most refractory sulfur-containing molecules) depends on the remaining, less efficient HYD pathway. HDS of 4,6-DMDBT is readily possible through the HYD pathway but is strongly hindered in the presence of amines. The strong negative influence of amines on the HYD pathway of the HDS of DBT and 4,6-DMDBT shows why the deep removal of sulfur from actual feeds is difficult. Optimum catalysts should be able to remove sulfur by hydrogenation not only in the presence of H<sub>2</sub>S, but also in the presence of amines and ammonia. Our results have demonstrated that the NiMo catalyst is much less sensitive to amines than the Mo and CoMo catalysts. At low concentrations, amines even promote the DDS pathway in the HDS of DBT over the NiMo catalyst.

Amines strongly decrease the HDS rate and especially the HYD rate. Geometric factors are held responsible for this inhibition. Amines adsorb in the  $\sigma$  mode through an interaction of their lone electron pair on the nitrogen atom with the catalyst surface. In their standing-up configuration, they hinder the flat  $\pi$  adsorption of the DBT and 4,6-DMDBT aromatic molecules and thus their hydrogenation. H<sub>2</sub>S has another inhibiting effect as well; it is small and does not constitute a large geometrical constraint, but fills sulfur vacancies at the catalyst surface. It thus diminishes the possibility of sulfur-containing molecules adsorbing with their S atom on a surface metal atom. Consequently, the DDS rate is decreased. HYD sites may not need sulfur vacancies; hydrogenation seems to occur over the whole edge surface on sites with and without sulfur vacancies. DDS sites, on the other hand, need vacancies. Consequently, vacancy sites are able to do hydrogenation as well as direct desulfurization, whereas fully covered sites can do only hydrogenation.

In explaining the behavior of the three catalysts, we relied on information derived from DFT calculations. But it should be noted that however useful these calculations are, they have been able to calculate the structure of the Mo, Co, and Ni atoms only at edges of the promoted and unpromoted MoS<sub>2</sub> crystallites. Currently, calculations of metal atoms at corner sites are too demanding, because of the low symmetry and thus large unit cells needed in the calculation. Consequently, such calculations have not yet been performed, and our knowledge about the role of corner sites in DDS or HYD reactions remains limited. Early literature suggested that bare corner sites allow the more space-demanding  $\eta^5$  and  $\eta^6$   $\pi$ -adsorption and thus would be good hydrogenation sites [41,42]. How stable such bare corner sites are in the presence of H<sub>2</sub>S and amines awaits future calculations.

## References

- [1] C.N. Satterfield, M. Modell, J.A. Wilkens, *Ind. Eng. Chem. Proc. Des. Dev.* 19 (1980) 154.
- [2] M. Nagai, T. Kabe, *J. Catal.* 81 (1983) 440.
- [3] M.J. Girgis, B.C. Gates, *Ind. Eng. Chem. Res.* 30 (1991) 2021.
- [4] D.D. Whitehurst, T. Isoda, I. Mochida, *Adv. Catal.* 42 (1998) 345.
- [5] M. Nagai, *Ind. Eng. Chem. Prod. Res. Dev.* 24 (1985) 489.
- [6] M. Nagai, T. Sato, A. Aiba, *J. Catal.* 97 (1986) 52.
- [7] V. La Vopa, C.N. Satterfield, *Chem. Eng. Commun.* 70 (1988) 171.
- [8] M. Nagai, *Chem. Lett.* 6 (1987) 1023.
- [9] M. Egorova, R. Prins, *J. Catal.* 221 (2004) 11.
- [10] M. Egorova, R. Prins, *Catal. Lett.* 92 (2004) 87.
- [11] M. Egorova, R. Prins, *J. Catal.* 224 (2004) 278.
- [12] M. Egorova, Y. Zhao, P. Kukula, R. Prins, *J. Catal.* 206 (2002) 263.
- [13] M. Houalla, N.K. Nag, A.V. Sapre, D.H. Broderick, B.C. Gates, *AIChE J.* 24 (1978) 1015.
- [14] M. Egorova, R. Prins, *J. Catal.* 225 (2004) 417.
- [15] D.H. Broderick, B.C. Gates, *AIChE J.* 27 (1981) 663.
- [16] M. Vrinat, L. de Mourgues, *J. Chem. Phys.* 79 (1981) 45.
- [17] Q. Zhang, W. Qian, A. Ishihara, T. Kabe, *Sekiyu Gakkaishi* 40 (1997) 185.
- [18] M. Vrinat, *Appl. Catal.* 6 (1983) 137.
- [19] V. Vanrysselberghe, G.F. Froment, *Ind. Eng. Chem. Res.* 35 (1996) 3311.
- [20] Y. Zhao, P. Kukula, R. Prins, *J. Catal.* 221 (2004) 441.
- [21] R. Prins, V.H.J. de Beer, G.A. Somorjai, *Catal. Rev.-Sci. Eng.* 31 (1989) 1.
- [22] R.R. Chianelli, M. Daage, M.J. Ledoux, *Adv. Catal.* 40 (1994) 177.
- [23] H. Topsøe, B.S. Clausen, F.E. Massoth, in: *Catalysis: Science and Technology*, vol. 11, Springer, Berlin, 1996.
- [24] L.S. Byskov, J.K. Nørskov, B.S. Clausen, H. Topsøe, *J. Catal.* 187 (1999) 109.
- [25] P. Raybaud, J. Hafner, G. Kresse, S. Kasztelan, H. Toulhoat, *J. Catal.* 189 (2000) 129.
- [26] P. Raybaud, J. Hafner, G. Kresse, S. Kasztelan, H. Toulhoat, *J. Catal.* 190 (2000) 128.
- [27] S. Cristol, J.F. Paul, E. Payen, D. Bougeard, S. Clémendot, F. Hutschka, *J. Phys. Chem. B* 104 (2000) 11220.
- [28] H. Schweiger, P. Raybaud, H. Toulhoat, *J. Catal.* 212 (2002) 33.
- [29] M. Sun, A.E. Nelson, J. Adjaye, *J. Catal.* 226 (2004) 32.
- [30] A. Travert, H. Nakamura, R.A. van Santen, S. Cristol, J.F. Paul, E. Payen, *J. Am. Chem. Soc.* 124 (2002) 7084.
- [31] J.F. Paul, E. Payen, *J. Phys. Chem. B* 107 (2003) 4057.
- [32] M. Sun, A.E. Nelson, J. Adjaye, *Catal. Today* 105 (2005) 36.
- [33] S. Cristol, J.F. Paul, E. Payen, D. Bougeard, F. Hutschka, S. Clémendot, *J. Catal.* 224 (2004) 138.
- [34] J.V. Lauritsen, S. Helveg, E. Lægsgaard, I. Stensgaard, B.S. Clausen, H. Topsøe, F. Besenbacher, *J. Catal.* 197 (2001) 1.
- [35] G.H. Singhal, R.L. Espino, J.E. Sobel, G.A. Huff, *J. Catal.* 67 (1981) 457.
- [36] F. Bataille, J.L. Lemberon, P. Michaud, G. Pérot, M.L. Vrinat, M. Lemaire, E. Schulz, M. Breysse, S. Kasztelan, *J. Catal.* 191 (2000) 409.
- [37] J. Mijoin, G. Pérot, F. Bataille, J.L. Lemberon, M. Breysse, S. Kasztelan, *Catal. Lett.* 71 (2001) 139.
- [38] T. Todorova, R. Prins, Th. Weber, *J. Catal.* 236 (2005) 190.
- [39] P. Kieran, C. Kember, *J. Catal.* 4 (1965) 380.
- [40] P. Kukula, A. Dutly, N. Sivasankar, R. Prins, *J. Catal.* 236 (2005) 14.
- [41] R.J.H. Voorhoeve, J.C.M. Stuijver, *J. Catal.* 23 (1971) 243.
- [42] T. Okuhara, K. I Tanaka, *J. Chem. Soc. Faraday Trans.* 75 (1979) 7.